ISSN 1063-7842, Technical Physics, 2013, Vol. 58, No. 7, pp. 1073–1079. © Pleiades Publishing, Ltd., 2013.
Original Russian Text © A.B. Rinkevich, V.V. Ustinov, L.N. Romashev, M.A. Milyaev, N.N. Sidun, E.A. Kuznetsov, 2013, published in Zhurnal Tekhnicheskoi Fiziki, 2013, Vol. 83, No. 7, pp. 146–152.

RADIOPHYSICS

# High-Frequency Properties of Fe/Cr Superlattices with Thin Cr Layers in the Millimeter-Wavelength Range

**A. B. Rinkevich[a]*, V. V. Ustinov[a], L. N. Romashev[a], M. A. Milyaev[a], N. N. Sidun[a], and E. A. Kuznetsov[b]**

[a] *Institute of Metal Physics, Ural Branch, Russian Academy of Sciences, ul. S. Kovalevskoi 18, Yekaterinburg, 620990 Russia*
[b] *Nizhni Tagil State Socio-Pedagogical Academy, ul. Krasnogvardeiskaya 57, Nizhni Tagil, 622031 Russia*
*e-mail: rin@imp.uran.ru*

Received September 14, 2012

**Abstract**—Microwave properties of Fe/Cr multilayer nanostructures with thin chromium layers (with thickness $t_{Cr} < 1$ nm) are analyzed. Experiments are performed by the method of penetration of microwaves in the frequency range from 26 to 38 GHz. The dependence of the transmission coefficient for microwaves on the constant magnetic field strength exhibits the microwave magnetoresistive effect and magnetic resonance. The resonance spectrum is reconstructed from measurements at various frequencies. The results of microwave measurements are analyzed together with the results of magnetic and magnetoresistive measurements.

**DOI:** 10.1134/S1063784213070177

## INTRODUCTION

Multilayer metal nanostructures with alternating ultrathin layers of ferromagnetic and "nonmagnetic" metals have become objects of detailed investigations of magnetic and magnetotransport properties. Analysis of multilayer nanostructures in which the ferromagnetic metal (component) is either in ultrathin layers near the percolation threshold or in the form of individual cluster islands distributed at random in the plane of the layer (cluster-layered nanostructures) is of special interest. Naturally, the magnetization curves for such nanostructures contain magnetic contributions both from the regions in the sample in which the magnetic ordering of adjacent layers of the ferromagnetic components is preserved and the regions containing only individual clusters of this component. The magnetic contributions from different regions of the nanostructure exhibit different dependences on the external magnetic field strength and are manifested not only in its magnetization, by also in the magnetoresistance [1–4].

It was shown in [5] that the magnetoresistance in the Fe/Cr cluster-layered nanostructures with a thickness of Fe layers below the percolation threshold is a linear function of the external magnetic field in a wide range of the external magnetic field and is almost independent of the field direction. Another unique feature of the Fe/Cr cluster-layered nanostructures with cluster-type Fe layers is that their temperature coefficient of the resistance may change its sign. With decreasing temperature, the resistivity of the nanostructure first decreases and then increases beginning with a certain critical temperature; at the helium temperature, its value can even be higher than at the initial (room) temperature. After the application of a magnetic field, the minimum on the temperature dependence of resistivity decreases and may disappear altogether in a high field strength like for alloys with the Kondo effect.

Multilayer metal nanostructures for which ultrathin (cluster) layers are formed from nonmagnetic metal (e.g., Fe/Cr superlattices with ultrathin Cr layers) are investigated less thoroughly. Nevertheless, analysis of magnetotransport properties of such nanostructures is also of interest due to the fact, for example, that the moduli of the bilinear and biquadratic exchange constants vary differently upon a decrease in the thickness of the nonferromagnetic metal layer. The magnetoresistance must change accordingly.

In this study, we investigate the magnetic, magnetoresistive, and high-frequency properties of Fe/Cr nanostructures with a thickness of Cr layers above and below the percolation threshold. The experiments with nanostructures with cluster-type Fe layers have shown [5] that the percolation threshold for the Fe/Cr structures grown by molecular-beam epitaxy is manifested for layer thicknesses of ~(0.4–0.5) nm and strongly depends on the quality of the substrate surface. Our choice of the system of Fe/Cr nanostructures with ultrathin Cr layers for high-frequency investigations was dictated by the fact that we had already studied in detail the microwave properties of Fe/Cr superlattices with continuous Fe and Cr layers. In microwave experiments performed in this study, we used the method of penetration of electromagnetic waves through the nanostructure, which was tested in out earlier studies [6, 7]. The main object of investigations of multilayer nanostructures with Cr layers hav-

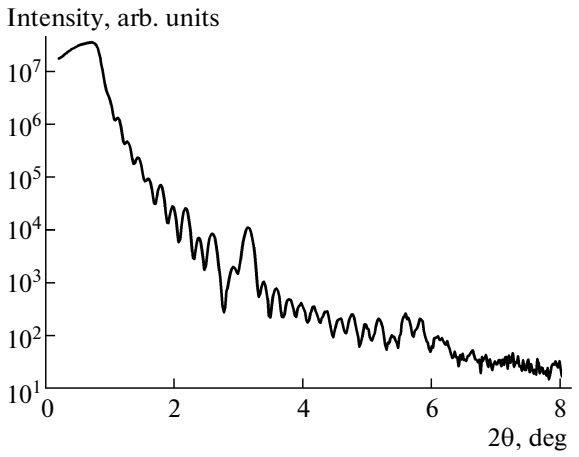


**Fig. 1.** Small-angle X-ray diffraction pattern of the $[Cr(0.7\ nm)/Fe(2.6\ nm)]_{12}/Cr(6.5\ nm)/Al_2O_3$ superlattice.

ing a thickness higher than the percolation threshold was the microwave giant magnetoresistive (GMR) effect. As regards experiments with nanostructures with a thickness of Cr layers below the percolation threshold, main attention was concentrated on analysis of the magnetic resonance because the GMR effect is not observed for such structures. We tried to find the dependence of the amplitude and width of the magnetic resonance line on the thickness of chromium layers, which can be treated as a nonmagnetic impurity in the ferromagnetic iron matrix in the case of small thicknesses. In this study, we used electromagnetic waves in the millimeter-wavelength range because the magnetic resonance is manifested most clearly during the penetration of these waves through the nanostructure.

## 1. CERTIFICATION OF SAMPLES

The experimental Fe/Cr nanostructures were grown by molecular-beam epitaxy in ultrahigh vacuum on single-crystal sapphire ($Al_2O_3$) substrates. To reduce the roughness of the substrate surface, a buffer layer of Cr atoms with a thickness of ~7 nm was formed on the substrate, after which Fe and Cr layers of the required thickness were grown successively on it. We prepared a batch of superlattices with a nominal thickness $t_{Cr}$ of chromium layers ranging from 0.4 to 2.5 nm and with the same thickness of iron layers in the interval 2.6–2.7 nm. The nominal thickness of the layers appearing in the formulas of nanostructures was calculated from the rate and time of their growth. In the prepared batch of superlattices, only two superlattices had thin (smaller that 0.9 nm) Cr layers. One of these superlattices, viz., $[Cr(0.7\ nm)/Fe(2.6\ nm)]_{12}/Cr(6.5\ nm)/Al_2O_3$, contained Cr layers with nominal thickness $t_{Cr} = 0.7$ nm, which is slightly higher than the percolation threshold amounting to ~0.5 nm (see above), while the other superlattice, $[Cr(0.45\ nm)/Fe(2.6\ nm)]_{12}/Cr(6.4\ nm)/Al_2O_3$, contained Cr layers with thickness $t_{Cr} = 0.45$ nm, which is slightly lower than the percolation threshold. Apart from superlattices, we prepared and tested the $Cr(1\ nm)/Fe(57.3\ nm)/Al_2O_3$ sample in the form of a 57.3-nm-thick Fe film protected from oxidation in air by a Cr layer (like superlattices). These three nanostructures were mainly used in our experiments.

One of the important problems to be solved in certification of superlattices is the determination of their atomic structure. In this study, the artificial periodicity produced in the nanostructure by alternating Fe and Cr layers was studied by small-angle X-ray diffraction on the DRON-3M diffractometer. The recording was performed in $CoK_\alpha$ radiation. By way of illustration of the spectra obtained in X-ray certification of nanostructures, Fig. 1 shows a typical X-ray reflectogram recorded on the superlattice sample $[Cr(0.7\ nm)/Fe(2.6\ nm)]_{12}/Cr(6.5\ nm)/Al_2O_3$. The singularities observed on the reflectogram near $2\theta \approx 3.2°$ indicate artificial periodicity of this nanostructure. The processing of X-ray data gives the value of the period of 3.4 nm, which coincides with the value calculated from the rate and time of layer formation. The spectrum also clearly demonstrates the presence of oscillations in the range of angles smaller than 3°. The existence of these oscillations indicates the sharpness of the boundaries between the Fe and Cr layers.

## 2. MAGNETIC AND MAGNETOREISTIVE PROPERTIES

To analyze the results of microwave measurements, we must know the magnetic state of nanostructures and their magnetization. This information was obtained by analysis of the magnetization isotherms measured by a high-sensitivity vibration magnetometer.

Figure 2a shows the magnetization curve for the $[Cr(0.7\ nm)/Fe(2.6\ nm)]_{12}/Cr(6.5\ nm)/Al_2O_3$ superlattice with thickness $t_{Cr} = 0.7$ nm of the Cr layers, which is slightly higher than the percolation threshold. Figure 2b shows the magnetization curve $[Cr(0.45\ nm)/Fe(2.6\ nm)]_{12}/Cr(6.4\ nm)/Al_2O_3$ nanostructure with $t_{Cr} = 0.45$ nm, which is slightly lower than the percolation threshold. Figure 2c shows for comparison the magnetization curve for the $Cr(1\ nm)/Fe(57.3\ nm)/Al_2O_3$ iron film. Comparing and analyzing the magnetization curves in Fig. 2, we can draw the following conclusions. The magnetization curve for the superlattice with $t_{Cr} = 0.7$ nm is typical of Fe/Cr nanostructures with a nonuniform magnetic ordering of Fe layers. In some regions of the sample of such a superlattice, the magnetic moments of adjacent Fe layers are ferromagnetically ordered, and magnetic saturation is attained in weak magnetic fields, while in other regions of the same sample, the magnetic moments of adjacent Fe layers are antiparallel or oriented at a certain angle to one another, and

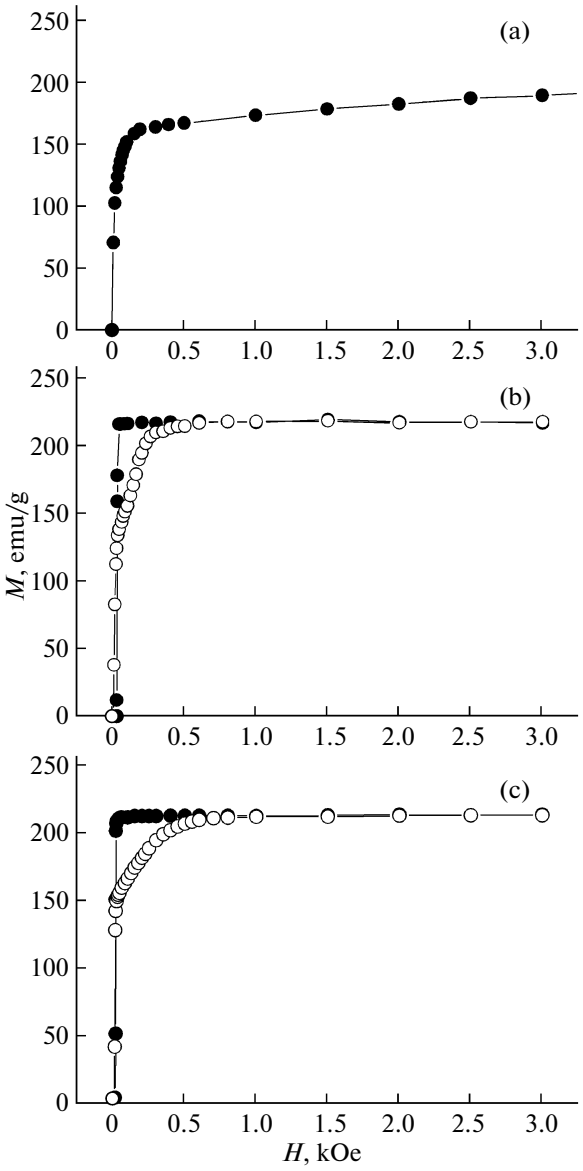


**Fig. 2.** Magnetization curves of (a) [Cr(0.7 nm)/Fe(2.6 nm)]$_{12}$/Cr(6.5 nm)/$Al_2O_3$, (b) [Cr(0.45 nm)/Fe(2.6 nm)]$_{12}$/Cr(6.4 nm)/$Al_2O_3$, and (c) Cr(1 nm)/Fe(57.3 nm)/$Al_2O_3$ nanostructures.

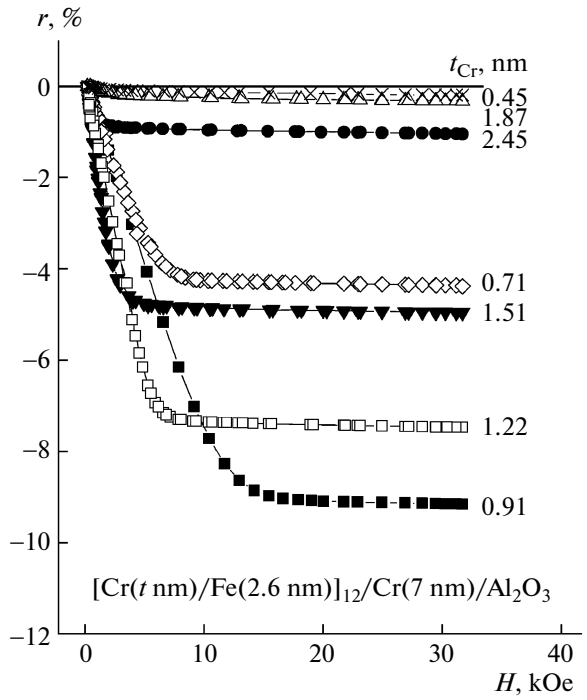


**Fig. 3.** Field dependences of the relative magnetoresistance of [Cr($t$ nm)/Fe(2.6 nm)]$_{12}$/Cr(7 nm)/$Al_2O_3$ nanostructures with different thicknesses $t_{Cr}$ of chromium layers.

magnetic saturation is attained in stronger fields; this is illustrated by the magnetization curve in Fig. 2a. Comparison of the magnetization curves obtained on the superlattice with $t_{Cr} = 0.45$ nm (Fig. 2b) and on the Fe film (Fig. 2c) shows their coincidence both in shape and in magnetic characteristics (in particular, in the saturation magnetization and saturation field). This experimentally observed magnetic similarity indicates that the superlattice with $t_{Cr} = 0.45$ nm is ferromagnetic like an ordinary Fe film, and the Cr layers with such a small nominal thickness in it are not continuous but consist of individual islands (clusters) distributed chaotically in the plane of the layer. The cluster state of Cr layers makes it possible for adjacent Fe layers to be connected by bridges (formed by Fe atoms) to ensure the ferromagnetic state in the structure as a whole.

Figure 3 shows the field dependences of the magnetoresistance of the Fe/Cr superlattices investigated in our experiments. The magnetoresistance was measured by the conventional four-contact method at room temperature in a constant magnetic field (of strength 32 kOe) directed parallel to the plane of the sample (film) and the current flowing in the sample. Relative magnetoresistance $r = [R(H) - R(0)]/R(0)$, where $R(H)$ is the sample resistance in magnetic field $H$, is laid on the ordinate axis in Fig. 3. It can be seen that the magnetoresistance of nanostructures considerably depends on the thickness of the Cr layers. It is well known that this dependence is oscillating by nature, and the maximal magnetoresistance (GMR effect) is observed for Fe/Cr superlattices with $t_{Cr} \sim$ (0.9–1.0) nm. The $r(t_{Cr})$ dependence obtained on Fe/Cr superlattices synthesized and tested in this study is shown in Fig. 4. The values of $r$ in Fig. 4 were obtained for $H = 32$ kOe, which corresponds to the magnetic saturation region.

Figures 3 and 4 show that the sample of the superlattice with $t_{Cr} = 0.7$ nm has a high relative magnetoresistance (~4.3%). This means that the Cr layers formed in this superlattice are continuous. As it regards the superlattice with $t_{Cr} = 0.45$ nm, its magnetoresistance is very low (in contrast to the first sample)

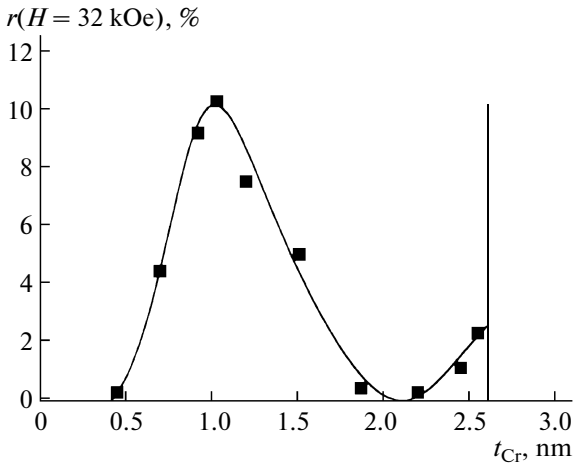


**Fig. 4.** Dependence of the relative magnetoresistance of $[Cr(t\ nm)/Fe(2.6\ nm)]_{12}/Cr(7\ nm)/Al_2O_3$ nanostructures, measured in field $\mathbf{H} = 32$ kOe, on the thickness $t_{Cr}$ of chromium layers.

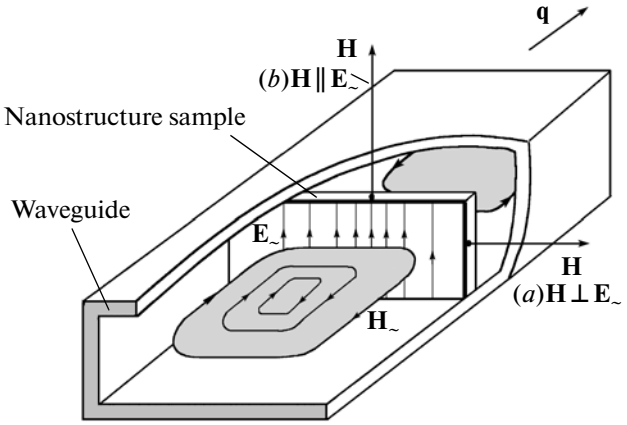


**Fig. 5.** Arrangement of the sample of a nanostructure in the waveguide for microwave measurements by the penetration method.

and amounts to only 0.2% in field $H = 32$ kOe. This means that the GMR effect in Fe/Cr superlattices with the thickness of the Cr layers lower than the percolation threshold is not observed.

## 3. RESULTS OF MICROWAVE MEASUREMENTS

In microwave measurements, we used the method of penetration of electromagnetic waves through a planar nanostructure, which was described in our earlier publications [8, 9]. The nanostructure sample is placed into a rectangular waveguide as shown in Fig. 5. The waveguide operates at the $TE_{10}$ mode. The directions of the microwave electric field $\mathbf{E}_\sim$ and microwave magnetic field $\mathbf{H}_\sim$ are shown by arrows. We implemented two variants of constant magnetic field $\mathbf{H}$: (a) $\mathbf{H}$ lies in the plane of $\mathbf{H}_\sim$ and (b) $\mathbf{H}$ is perpendicular to the $\mathbf{H}_\sim$ plane. The electromagnetic wave incident on the sample with a planar metallic nanostructure is partly reflected and partly transmitted through it. In the penetration method, the modulus of the transmission coefficient is measured as a function of the constant magnetic field strength $|D(H)|$. We calculated the relative variation in the modulus of transmission coefficient ($r_m = [|D(H)| - |D(0)|]/|D(0)|$).

The experiments were carried out in the frequency range $f = 26$–$38$ GHz. The results of analysis of the microwave GMR effect in superlattices with thin Cr layers are represented in Fig. 6. Figure 6a shows the results of measurements of this effect in the $[Cr(0.7\ nm)/Fe(2.6\ nm)]_{12}/Cr(6.5\ nm)/Al_2O_3$ nanostructure. Measurements were taken at several frequencies with the vector of the constant magnetic field lying in the plane of the microwave field. Such a variant of the arrangements of the fields is chosen to exclude the effect of magnetic resonance on the results. The results shown in Fig. 6a indicate that the microwave GMR effect depends on the electromagnetic wave frequency only slightly. We have observed the same situation earlier on Fe/Cr superlattices with continuous layers [7]. The results of microwave measurements for two orientations of the constant magnetic field for the same nanostructure are compared in Fig. 6b. In the case when $\mathbf{H}$ is perpendicular to the plane of field $\mathbf{H}_\sim$, the resonance minimum caused by the magnetic resonance is observed apart from the GMR effect. Comparison of the field dependences of the microwave transmission coefficient $r_m$ and relative magnetoresistance $r$ obtained on the same $[Cr(0.7\ nm)/Fe(2.6\ nm)]_{12}/Cr(6.5\ nm)/Al_2O_3$ sample is illustrated in Fig. 6c. It can be seen that these dependences are identical in shape, but the relative magnetoresistance measured in direct current considerably exceeds the relative variation in the modulus of the microwave transmission coefficient.

The magnetoresistance of the $[Cr(0.45\ nm)/Fe(2.6\ nm)]_{12}/Cr(6.4\ nm)/Al_2O_3$ nanostructure is very small; therefore, we cannot expect a high microwave magnetoresistance for this structure. Comparing the results of microwave measurements on this nanostructure with the results obtained on the $Cr(1\ nm)/Fe(5.73\ nm)/Al_2O_3$ iron film (see Fig. 7), we note that both nanostructures do not exhibit the GMR effect; however, variations of the resonance type are clearly manifested. These variations for the iron film (Fig. 7a) in the frequency range under investigation are in the range of 10–30%, while these variations for the $[Cr(0.45\ nm)/Fe(2.6\ nm)]_{12}/Cr(6.4\ nm)/Al_2O_3$ superlattice are much smaller (0.7–1.7%). In both nanostructures, resonance field $H_{RES}$ increases with frequency. By measuring the resonance field at several frequencies, we can reconstruct the resonance spectrum. The results obtained for the three nanostruc-

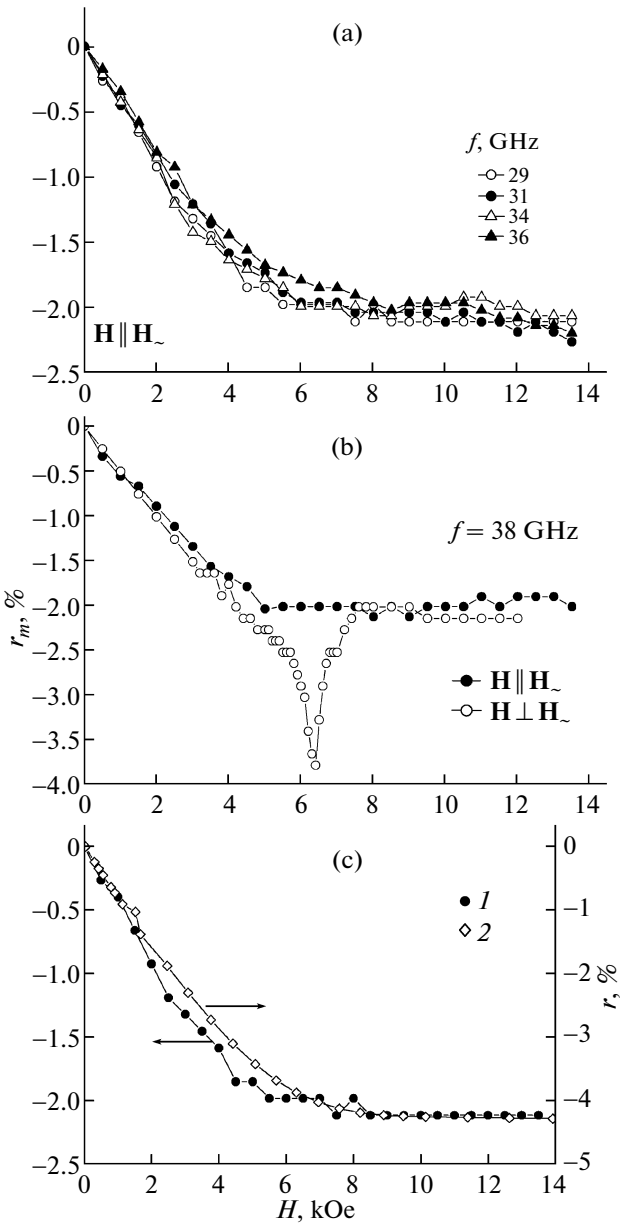


**Fig. 6.** (a) Field dependences of the coefficient of transmission through the $[Cr(0.7\ nm)/Fe(2.6\ nm)]_{12}/Cr(6.5\ nm)/Al_2O_3$ nanostructure measured at several frequencies for $\mathbf{H} \parallel \mathbf{H}_{\sim}$; (b) microwave GMR effect and magnetic resonance in the same nanostructure; and (c) comparison of the microwave magnetoresistance (*1*) and magnetoresistance (*2*) measured in direct current.

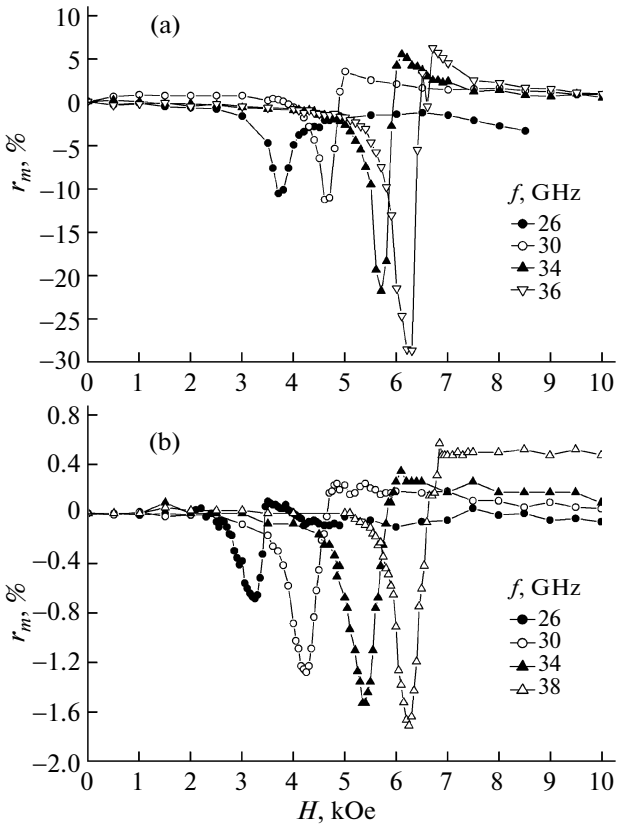


**Fig. 7.** Magnetic resonance in the penetration of electromagnetic waves. Field dependence of the coefficient of transmission of electromagnetic waves through (a) $Cr(1\ nm)/Fe(57.3\ nm)/Al_2O_3$ iron film and (b) $[Cr(0.45\ nm)/Fe(2.6\ nm)]_{12}/Cr(6.4\ nm)/Al_2O_3$ superlattice.

tures are shown in Fig. 8. The variations in the transmission coefficient of the resonance type are observed for field **H** perpendicular to the plane of $\mathbf{H}_{\sim}$. Proceeding from this fact and from the dependence $H_{RES}(f)$, we can conclude that the observed minimum of the transmission coefficient is associated with uniform magnetic resonance. Comparison of the experimental and calculated resonance spectra will be carried out below.

## 4. DISCUSSION

The results of X-ray studies demonstrate artificial periodicity in the experimental samples. The results of magnetic and magnetoresistive measurements lead to the conclusion about the inhomogeneous magnetic state of nanostructures. The results indicate that the thickness of the Cr layers in the $[Cr(0.7\ nm)/Fe(2.6\ nm)]_{12}/Cr(6.5\ nm)/Al_2O_3$ nanostructure is higher than the percolation threshold, while Cr layers in the $[Cr(0.45\ nm)/Fe(2.6\ nm)]_{12}/Cr(6.4\ nm)/Al_2O_3$ nanostructure are not continuous. The regions in which the continuity is violated are filled with Fe atoms, and this leads to ferromagnetic ordering of adjacent Fe layers and the nanostructure as a whole.

Let us consider the typical features of the microwave properties of Fe/Cr nanostructures with thin Cr layers. Like in nanostructures with continuous layers, there are two physical reasons for variations in the microwave transmission coefficient. One of these reasons is a microwave analog of the giant magnetoresistance effect. It is observed irrespective of whether the direction of constant magnetic field **H** is parallel or perpendicular to the plane of microwave magnetic

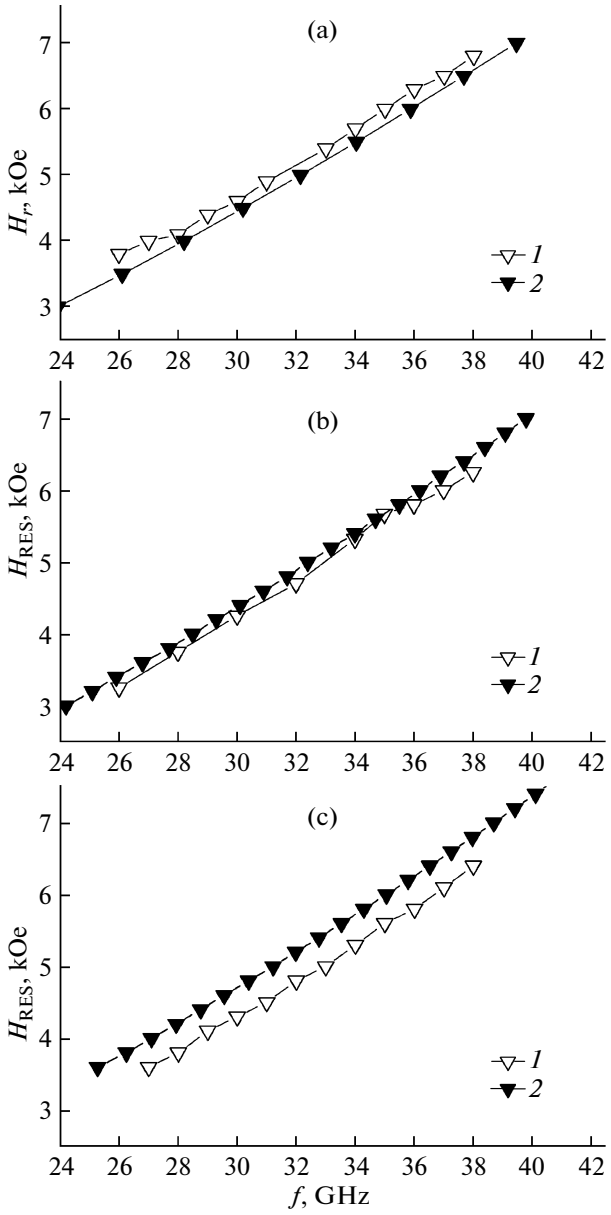


**Fig. 8.** Magnetic resonance spectra in the penetration of electromagnetic waves through (a) Cr(1 nm)/Fe(57.3 nm)/$Al_2O_3$, (b) [Cr(0.45 nm)/Fe(2.6 nm)]$_{12}$/Cr(6.4 nm)/$Al_2O_3$, and (c) [Cr(0.7 nm)/Fe(2.6 nm)]$_{12}$/Cr(6.5 nm)/$Al_2O_3$ nanostructures: *1*—experiment; *2*—calculations.

field $\mathbf{H}_{\sim}$. The magnetoresistance of metallic multilayer nanostructures is negative, and the coefficient of transmission of microwaves also decreases in a magnetic field due to the GMR effect. It is shown that the relative variation of the microwave transmission coefficient is much smaller than the relative magnetoresistance measured in direct current ($r_m < r$), but exhibits an analogous field dependence. The observed variations in the transmission coefficients due to the GMR effect in the nanostructures under investigation exhibit a weak frequency dependence. Analogous features were also observed in Fe/Cr superlattices with continuous layers investigated earlier, as well as in cluster-layered nanostructures with ultrathin Fe layers. The magnitude of the microwave GMR effect, as well as the magnetoresistive effect, is much weaker for nanostructures with ultrathin Cr layers than in nanostructures with continuous Cr layers and antiferromagnetic ordering of adjacent Fe layers.

The second reason for the observed microwave variations of the transmission coefficient is associated with changes in the surface impedance of the nanostructure under magnetic resonance conditions. Resonance-type variations of the transmission coefficient were observed experimentally in nanostructures with thin Cr layers when constant magnetic field **H** was perpendicular to the plane of microwave field $\mathbf{H}_{\sim}$. The amplitude of resonant variations of the transmission coefficient for nanostructures with $d_{Cr} = 0.70$ and 0.45 nm is much smaller than for Fe films. In our experiments, magnetic resonance was observed under the conditions of magnetic saturation of the samples. The resonance line width for the Cr(1 nm)/Fe(57.3 nm)/$Al_2O_3$ iron film is only slightly smaller than for superlattices with ultrathin Cr layers. This forms a considerable difference from superlattices with ultrathin Fe layers. The resonance line width for the latter superlattices is several times larger than for nanostructures with continuous layers [9]. In addition, the magnetic resonance observed in these superlattices at frequencies 26–38 GHz corresponds to an unsaturated state. The reason for this difference lies in peculiarities of the magnetic state of nanostructures. In particular, the large width of the magnetic resonance line for superlattices with ultrathin Fe layers is due to inhomogeneities in the magnetization of discontinuous layers and individual Fe clusters. The magnetization of superlattices with ultrathin Cr layers is much more uniform.

Let us analyze the results of measurements of the magnetic resonance spectra shown in Fig. 8. It has been established earlier that nanostructures exhibit the resonance belonging to the homogeneous acoustic branch in the magnetic resonance spectrum. It was shown in [10] that the spectrum of the acoustic branch can be calculated using the conventional Kittel formula

$$\omega = \gamma[H(H + 4\pi M_s)]^{1/2}, \qquad (1)$$

if $H > H_s$. In formula (1), $\omega = 2\pi f$ is the circular frequency, $\gamma$ is the magnetomechanical ratio, and $M_s$ is the saturation magnetization. If we use the results obtained above for the saturation magnetization, we can calculate the resonance spectrum in the form of the $H_{RES}(f)$ dependence and compare the calculated dependences with experimental curves (Fig. 8). For the Cr(1 nm)/Fe(57.3 nm)/$Al_2O_3$ iron film and the [Cr(0.45 nm)/Fe(2.6 nm)]$_{12}$/Cr(6.4 nm)/$Al_2O_3$ nanostructure, good agreement between the calculated and measured spectra is observed. The discrep-

ancy between the calculated and experimental spectra exceeding the errors is observed for the $[Cr(0.7\ nm)/Fe(2.6\ nm)]_{12}/Cr(6.5\ nm)/Al_2O_3$ nanostructure. For a certain fixed frequency, the experimental resonance field for this nanostructure turned out to be smaller than the calculated field. In accordance with formula (1), this corresponds to the situation in which the magnetization acting on microwaves is higher than the static magnetization. This fact contradicts, for example, the existence of "magnetically dead" layers in which atoms of the nominally ferromagnetic component in the interfaces make a smaller contribution to the magnetization [11, 12]. One of the possible explanations of the observed higher magnetization is that the magnetic moment of atoms in the interfaces can be higher than its conventional value [13].

## CONCLUSIONS

We have analyzed the magnetic, magnetoresistive, and microwave properties of Fe/Cr multilayer nanostructures with thin Cr layers, which are prepared by molecular beam epitaxy. It is shown that nanostructures with a thickness of Cr layers from 0.45 to 0.70 nm have a periodic structure and the continuity of Cr layers with $t_{Cr} = 0.45$ nm is broken. Upon an increase in the nominal width of Cr layers, the initially antiferromagnetic ordering of adjacent Fe layers (with $t_{Cr} \sim 0.9$ nm) becomes ferromagnetic for $t_{Cr} = 0.45$ because of the violation of the continuity of Cr layers alternating with Fe layers. Microwave measurements of the transmission coefficient confirm the existence of the microwave giant magnetoresistive effect for this type of nanostructures. The magnitude of this effect is smaller than the relative magnetoresistance measured in the same fields in direct current.

In Fe/Cr nanostructures with ultrathin Cr layers, magnetic resonance in the penetration of microwaves is observed. The amplitude of resonant variations in such nanostructures is much smaller than in a Fe film. The magnetic resonance line width for cluster-layered superlattices with Cr clusters is smaller than for superlattices with Fe clusters. The spectrum is reconstructed from the measurements of the magnetic resonance field. For the $[Cr(0.45\ nm)/Fe(2.6\ nm)]_{12}/Cr(6.4\ nm)/Al_2O_3$ cluster-layered nanostructure, the calculated spectrum of uniform resonance is in good agreement with the experimental spectrum. For the $[Cr(0.7\ nm)/Fe(2.6\ nm)]_{12}/Cr(6.5\ nm)/Al_2O_3$ nanostructure, the calculated and experimental spectra are different, the discrepancy being due to the fact that the effective magnetization forming the resonance condition is higher than the measured static magnetization.

## ACKNOWLEDGMENTS

This study was supported financially in part by the Russian Foundation for Basic Research (project no. 10-02-00590) and the program of the Presidium of the Russian Academy of Sciences.

## REFERENCES

1. R. Schad, C. D. Potter, P. Bellien, G. Verbanck, V. V. Moshchalkov, and Y. Bruynseraede, Appl. Phys. Lett. **64**, 3500 (1994).
2. T. Lucinski, D. Elefant, G. Reiss, and P. Verges, J. Magn. Magn. Mater. **162**, 29 (1996).
3. Chen Xu and Zhen-Ya Li, J. Magn. Magn. Mater. **206**, 113 (1999).
4. F. Spizzo, E. Angeli, D. Bisero, P. Vavassori, and F. Ronconi, J. Magn. Magn. Mater. **242–245**, 473 (2002).
5. V. V. Ustinov, L. N. Romashev, M. A. Milyaev, A. V. Korolev, T. P. Krinitsina, and A. M. Burkhanov, J. Magn. Magn. Mater. **300**, 148 (2006).
6. V. V. Ustinov, A. B. Rinkevich, L. N. Romashev, and V. I. Minin, J. Magn. Magn. Mater. **177–181**, 1205 (1998).
7. A. B. Rinkevich, L. N. Romashev, and V. V. Ustinov, JETP **90**, 834 (2000).
8. V. V. Ustinov, L. N. Romashev, V. I. Minin, A. V. Semerikov, and A. R. Del', Fiz. Met. Metalloved. **80** (2), 71 (1995).
9. V. V. Ustinov, A. B. Rinkevich, L. N. Romashev, M. A. Milyaev, A. M. Burkhanov, N. N. Sidun, and E. A. Kuznetsov, Fiz. Met. Metalloved. **99** (5), 44 (2005).
10. A. B. Drovosekov, O. V. Zhotikova, N. M. Kreines, V. F. Meshcheryakov, M. A. Milyaev, L. N. Romashev, V. V. Ustinov, and D. I. Kholin, JETP **89**, 986 (1999).
11. D. Labergerie, K. Westerholt, H. Zabel, and B. Hjörvarsson, I. Minin, J. Magn. Magn. Mater. **225**, 373 (2001).
12. A. B. Rinkevich, L. N. Romashev, M. A. Milyaev, V. V. Ustinov, and E. A. Kuznetsov, in *Proceedings of the 11th International Summer School Magnetic Nanostructures, Madrid, Spain, 2004.*
13. Z. Celinski, K. B. Urquhart, and B. Heinrich, J. Magn. Magn. Mater. **166**, 6 (1997).

*Translated by N.V. Wadhwa*